Rat Cavernous Nerve Reconstruction with CD133+ Cells Derived from Human Bone Marrow

Katsutoshi Miyamoto, MD, Shogo Inoue, MD, Kanao Kobayashi, MD, Mitsuru Kajiwara, MD, PhD, Jun Teishima, MD, PhD, and Akio Matsubara, MD, PhD

Department of Urology, Institute of Biomedical & Health Sciences, Hiroshima University, Hiroshima, Japan

ABSTRACT

Introduction. Erectile dysfunction remains a major complication after surgery of pelvic organs, especially after radical prostatectomy.

Aim. The aim of this study was to assess the effect of endothelial progenitor cells on the regeneration of cavernous nerves in a rat injury model.

Methods. A 2 mm length of the right and left cavernous nerves of 8-week-old male nude rats were excised. Alginate gel sponge sheets supplemented with 1×10^4 CD133+ cells derived from human bone marrow were then placed over the gaps on both sides (CD group). The same experiments were performed on sham-operated rats (SH group), rats with only the nerve excision (EX group), and rats with alginate gel sheets placed on the injured nerves (AL group).

Main Outcome Measures. Immunofluorescence staining and molecular evaluation were performed 4 days later. Functional and histological evaluations were performed 12 weeks later.

Results. The intracavernous pressure elicited by electrical stimulation and the neuronal nitric oxide synthase-positive area in surrounding tissues of the prostate was significantly greater in the CD group. Immunofluorescence microscopy showed that CD133+ cells were assimilated as vascular endothelial cells, and the real-time polymerase chain reaction showed upregulation of nerve growth factor and vascular endothelial growth factor in the alginate gel sponge sheets of the CD group.

Conclusions. Transplantation of CD133+ cells accelerated the functional and histological recovery in this cavernous nerve injury model, and the recovery mechanism is thought to be angiogenesis and upregulation of growth factors. CD133+cells could be an optional treatment for cavernous nerve injury after prostatectomy in clinical settings. **Miyamoto K, Inoue S, Kobayashi K, Kajiwara M, Teishima J, and Matsubara A. Rat cavernous nerve reconstruction with CD133+ cells derived from human bone marrow. J Sex Med **;**:**–**.**

Key Words. Cavernous Nerve; CD133+; Erectile Dysfunction; Radical Prostatectomy; Alginate Sheet; Cell Therapy

Introduction

Erectile dysfunction (ED) is one of the major complications for men who undergo radical prostatectomy because this surgical procedure frequently causes cavernous nerve injury. Although nerve-sparing techniques have made amazing strides, even when bilateral nerve-sparing techniques are used, the percentage of sexually active men retaining sexual potency after radical prostatectomy ranges from 31% to 86% [1]. Autologous nerve interposition grafting can prevent postoperative ED in prostate cancer patients who require wide resection of the prostate with neurovascular bundles, but among its many disadvantages are permanent loss of sensation, scar formation at the denervated sites, and the limited availability of donor nerves. Furthermore, the potency rates following the nerve-grafting operation are 31–43% [2] [3].

Many investigators have been studying the potential of cavernous nerve regeneration by using

animal models of ED. A biodegradable conduit graft and collagen sponge [4], glial cell-derived neurotrophic factor-transduced Schwann cell-seeded silicon tubes [5], and an alginate gel sponge sheet [6] have been used to regenerate injured nerves.

In the present study, we used human-derived CD133^{+} cells, which are a subset of CD34^{+} cells and have a very high potential for proliferation and differentiation [7], to regenerate cavernous nerves in a rat model. This is the first time these cells have been used in nerve regeneration studies, and here we show these cells strongly stimulate cavernous nerve regeneration by inducing angiogenesis.

Methods

Animals

We used 8-week-old male athymic nude rats (F344/N Jcl rnu/rnu, CLEA Japan, Inc., Tokyo, Japan) weighing 230–250 g and prepared a total of 36 rats. Twenty-eight rats were divided into four groups of seven each and assessed at 12 weeks later for functional and histological evaluation. Six rats were divided into two groups of three each and assessed at 4 days later for molecular evaluation, and two rats were assessed at 4 days later for histological evaluation. All the animal procedures were approved by the Animal Care and Animal Use committees of Hiroshima University.

CD133^{+} Cells and Alginate Gel Sponge Sheet

CD133^{+} cells derived from human bone marrow were purchased from Lonza (Walkersville, MD, USA). Just before use, they were thawed according to the manufacturer's instruction and resuspended in phosphate-buffered saline (PBS) at a concentration of 1×10^4 cells per 40 μL. Alginate gel sponge sheets were supplied by Koyo Sangyo, Tokyo, Japan.

Antibodies for Immunostaining

We used antibodies for neuronal nitric oxide synthase (nNOS) (Cell Signaling Technology, Inc., Danvers, MA, USA) and S100 protein (Dako, Carpinteria, CA, USA) to detect neuron tissue. nNOS is specific to cavernous nerve fiber, and S100 is specific to Schwann cells. We also used antibody for von Willebrand factor (vWF) (Dako) and α-smooth muscle actin (αSMA) (Dako) to find endothelial cells or blood vessels, and used anti-human nuclear antigen (HNA) antibody (Chemicon International, Temecula, CA, USA) to

find human-derived cells. The secondary antibodies were as follows: Alexa-conjugated goat anti-mouse immunoglobulin G (IgG) (Molecular Probes, Eugene, OR, USA) for HNA and αSMA, and Alexa-conjugated goat anti-rabbit IgG (Molecular Probes) for nNOS, S100, and vWF protein.

Surgical Procedures

The rats were anesthetized with pentobarbital sodium (50 mg/kg, intraperitoneally). A lower abdominal midline incision was made from the symphysis pubis to mid-abdomen. Then on the right and left sides of the prostate, the major pelvic ganglion (MPG) and the cavernous nerves extending from it to the penis were identified and exposed under magnification (Step 1). The rats undergoing only this procedure were designated to the sham (SH) group. Then on both sides, a 2 mm length between the MPG and penile base was excised from the cavernous nerves with micro-scissors (Step 2). The rats undergoing only the Step 1 and Step 2 procedures were designated to the excision (EX) group. Then a 4 mm × 4 mm alginate gel sponge sheet was placed, without suturing, over the gap between the stumps of the cavernous nerves (Step 3). The rats undergoing only the Step 1, Step 2, and Step 3 procedures were designated to the alginate (AL) group. Finally, CD133^{+} cells (1×10^4/40 μL PBS) were dropped onto the sheet (Step 4). The rats undergoing all four of these procedures were designated to the CD133^{+} (CD) group.

Evaluation of Erectile Function

Twelve weeks after the above surgery, 7 rats (14 study nerves) in each group again received pentobarbital anesthesia. The right and left MPG were exposed as described above, and a 23G needle was inserted into the penile crus, filled with 250 U/mL heparin solution, and connected to a pressure transducer for intracavernous pressure (ICP) measurement. A 24G polyethylene cannula filled with 250 U/mL heparin solution was inserted into the right femoral artery and connected to a pressure transducer for monitoring arterial pressure (AP). Electrical stimulation (0.5 mA and 20 Hz for 1 minute) was applied to the MPG on each side by using a bipolar hook electrode connected to an electrostimulator (Unique Acquisition version 3, Unique Medical, Tokyo, Japan). On each side, the ICP and AP during the electrostimulation were measured simultaneously, and the maximal ICP divided by the mean AP (ICP/MAP) was calculated.

The mean ICP/MAP for a total of 14 sides was then compared among the four groups.

Morphologic Analysis
After the evaluation of erectile function, prostates were harvested en bloc with surrounding tissues from two rats (four study nerves) in each group and placed in 10% neutral-buffered formalin. The tissues were embedded in paraffin and cut into 4 µm thick sections at 20 µm intervals. The sections at the intermediate portion between the MPG and penile base were then stained with hematoxylin-eosin (HE) and observed by light microscopy.

Immunohistochemical Analysis of Nerve Regeneration and Angiogenesis
Frozen sections were prepared for immunohistochemical analysis. As in the analysis with HE staining, prostates were harvested en bloc with surrounding tissues from two rats (four study nerves) in each group. The harvested tissues were fixed in 4% paraformaldehyde for about 48 hours and then immersed in a series of increasing concentrations (10%, 20%, and 30% wt/vol) of sucrose in PBS. They were then embedded in freezing medium (optimal cutting temperature compound, Sakura Finetek, Torrance, CA, USA) and frozen in liquid nitrogen at –80°C. Transverse sections 8 µm thick were serially sliced on a cryostat at intervals of 40 µm. Sections at the intermediate portion between the MPG and penile base were thaw-mounted on Matsunami adhesive silane-coated glass slides and air dried. After the sections were treated with blocking solution (Protein Block Serum-Free, Dako) for 30 minutes, antibodies for nNOS (1:200), or vWF (1:100) and αSMA (1:100) were applied. Alexa-conjugated goat anti-rabbit IgG (1:500) and Alexa-conjugated goat anti-mouse IgG (1:500) were used as the secondary antibodies. A 4′,6-diamidino-2-phenylindole solution was also applied for 5 minutes for nuclear staining. Coverslips were attached to the slides by using Fluoromount mounting medium (Diagnostic BioSystems, Pleasanton, CA, USA).

Five serial sections were selected from the portion where cavernous nerves had been excised, and nNOS-positive cells, vWF-positive cells, and αSMA-positive cells were observed using a fluorescence microscope (BZ-8100, Keyence Corporation, Osaka, Japan). We then measured the total nNOS-positive area in each section by using image analysis software (NIH Image, National Institutes of Health, Bethesda, MD, USA) and calculated the mean value for 20 portions (5 serial sections × 2 rats × right and left sides). For the AL group and CD group, we also evaluated blood vessel density in surrounding tissues of the prostate that included an alginate sponge gel sheet. The number of blood vessels, which were defined as circular or ovoid structures surrounded by vWF- and αSMA-positive blood vessel, was calculated and divided by the total area of the surrounding prostate tissue. The mean value for 20 portions was compared between the two groups.

To assess how the transplanted human-derived CD133⁺ cells had differentiated, we separately harvested prostate tissue en bloc in the CD group at 4 days (two rats, four study nerves) and 12 weeks (three rats, six study nerves) after the transplantation of CD133⁺ cells. Using five serial sections at the intermediate portion between the MPG and penile base, we evaluated staining properties for nNOS (1:200), S100 (1:200), vWF (1:100), and HNA (1:50) with a fluorescence microscope.

Reverse Transcription-Polymerase Chain Reaction
In the AL and CD groups, 4 days after the nerve segments were excised and an alginate gel sheet was placed over the nerve stumps, the sheets on both sides of the prostate were retrieved from three rats (six sheets in total) in each group. They were quickly frozen in liquid nitrogen and stored at –80°C. The first-strand cDNAs were synthesized from the total RNAs isolated from the stored samples by using the RNeasy Mini Kit (QIAGEN, Germantown, MD, USA) and First-Strand cDNA Synthesis Kit (GE Healthcare Life Sciences, Uppsala, Sweden). Then cDNAs for human vascular endothelial growth factor (VEGF), rat VEGF, rat nerve growth factor (NGF), human glyceraldehyde 3-phosphate dehydrogenase (GAPDH), and rat β-actin were amplified by Taq DNA polymerase (Applied Biosystems, Foster City, CA, USA) under the following condition: 35 cycles of 30 seconds of initial denaturation at 94°C, annealing at 56°C for 30 seconds, and 1 minute of extension at 72°C. The primer pairs are listed in Table 1. Reverse transcription-polymerase chain reaction (RT-PCR) products were electrophoresed in a 2% agarose gel containing ethidium bromide in Tris-borate-ethylenediaminetetraacetic acid electrophoresis buffer and were visualized by ultraviolet transillumination.

For quantitative analysis of the above intrinsic growth factors, quantitative RT-PCR was performed with a 7900HT Fast Real-Time PCR

Table 1 Characteristics of primers used in this study

Gene	Primer pair sequence	Fragment length (bp)
hVEGF	F:5′-GGGCAGAATCATCACGAAGT-3′ R:5′-GCGGCAGCGTGGTTT-3′	202
hGAPDH	F:5′-TCCCATCACCATCTTCCA-3′ R:5′-CATCACGCCACAGTTTCC-3	380
rNGF	F:5′-AGGGCAGACCCGCAACATC-3′ R:5′-GGTGGAGGCTGGGTGCTAAAC-3′	93
rVEGF	F:5′-TACCTCCACCATGCCAAGTG-3′ R:5′-TCTGCTCCCCTTCTGTCGTG-3′	55
rβ-actin	F:5′-GATCATTGCTCCTCCTGAGCG-3′ R:5′-TGCTGATCCACATCTGCTGGA-3′	92

hGAPDH = human glyceraldehyde 3-phosphate dehydrogenase; *hVEGF* = human vascular endothelial growth factor; *rβ-actin* = rat β-actin; *rNGF* = rat nerve growth factor; *rVEGF* = rat vascular endothelial growth factor

System (Applied Biosystems) using SYBR Green PCR Core Reagents (Applied Biosystems) according to the manufacturer's protocol. Relative quantification of target gene expression was calculated using the comparative cycle threshold method, and β-actin was used as an endogenous control. Mean values of six samples were calculated and compared between the two groups.

Statistical Analysis

All values were expressed as mean ± standard errors. The Kruskal–Wallis test with a Steel-Dwass post hoc test was used to assess the ICP/MAP values and the total nNOS-positive areas, and the Mann–Whitney U-test was used to assess

blood vessel densities and mRNA expression levels. Significance was set at $P < 0.05$.

Results

Restoration of Erectile Function

ICP and MAP were measured for the purpose of assessing erectile function. Representative changes in ICP and AP are shown in Figure 1A. While no ICP increase elicited by electrical stimulation was observed in the EX group, there were obvious responses in other groups. The mean ICP/MAP for 14 portions of the CD group (0.57 ± 0.07) was significantly higher than that of the EX group (0.31 ± 0.05) ($P = 0.04$), and similar to that of the SH group (0.67 ± 0.05). Also, there was no significant difference between AL group (0.38 ± 0.06) and EX group (Figure 1B). Erectile function of cell treated group recovered to the level of sham group.

Histological Analysis for Nerve Regeneration

Figure 2A shows micrographs of the prostate and surrounding tissues harvested 12 weeks after surgery. HE staining indicated apparent nerve tissues adjacent to the prostate in the SH, AL, and CD groups (red arrows in the middle row of panels in Figure 2A) but not in the EX group. This was evidenced by immunofluorescence microscopy. While nNOS-positive areas (green regions indi-
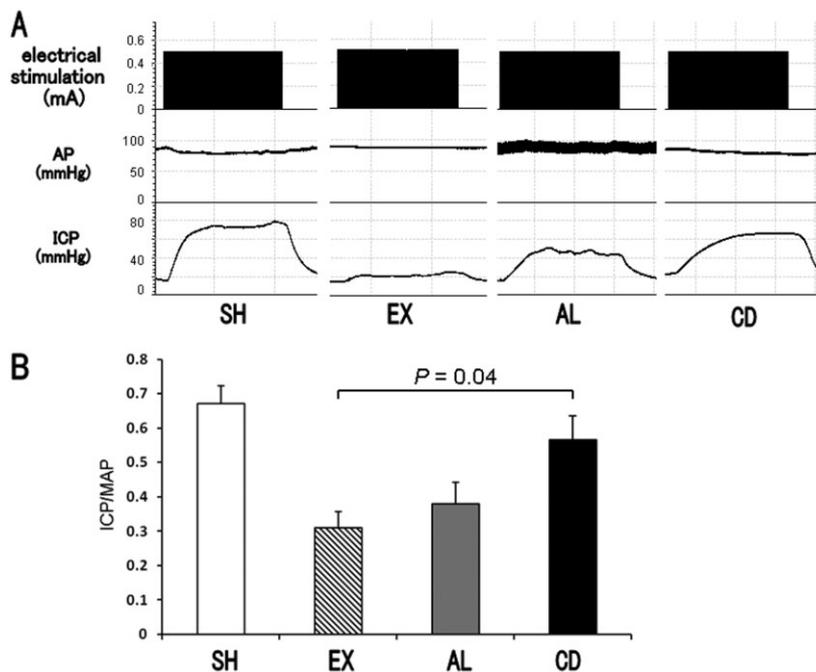

Figure 1 Intracavernous pressure (ICP) and arterial pressure (AP) response elicited by MPG electrical stimulation (0.5 mA and 20 Hz for 1 minute) 12 weeks later. (A) Representative findings. (B) Mean ICP/mean arterial pressure (MAP). Boxes show mean value for each group, and error bars show standard error. AL = alginate group; CD = CD133+ group; EX = excision group; SH = sham group.
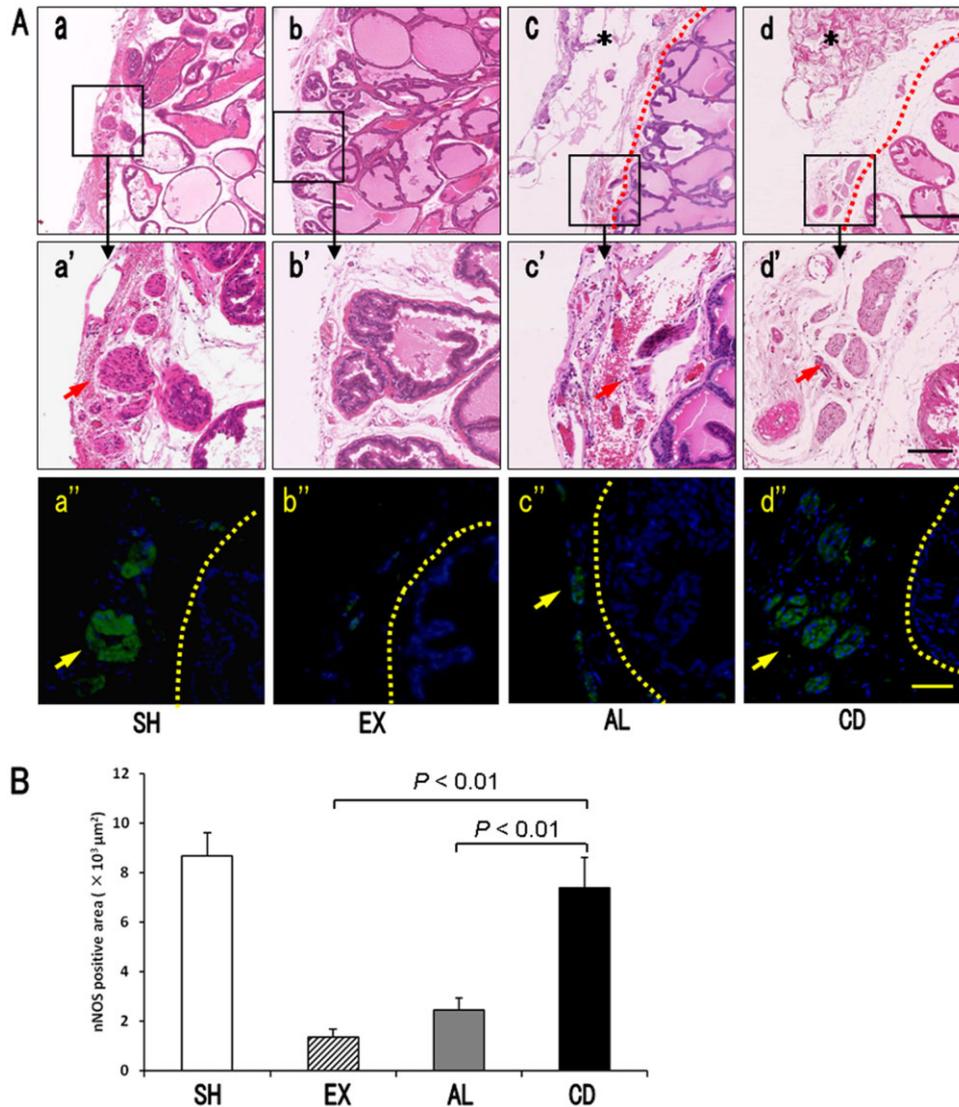
Figure 2 Nerve tissues in surrounding tissues of prostate at 12 weeks. (A-a, b, c, d) Representative light micrographs showing HE-stained harvested tissues. Bar = 200 μm. (A-a′, b′, c′, d′) Magnified zones of A-a, b, c, d. Bar = 100 μm. (A-a″, b″, c″, d″) Representative fluorescence micrographs showing neuronal nitric oxide synthase (nNOS) (green) and DAPI (blue). Bar = 100 μm. Nerve tissues in SH group, AL group, and CD group are shown by arrows. Only a little nerve tissue was seen in the EX group (A-b, b′, b″). Alginate gel sponge sheets were observed in the AL group and CD group (asterisks). Prostate tissue and surrounding tissue of prostate are separated by red dotted lines in A-c and A-d. A-a″, b″, c″, d″ are divided into two regions by dotted lines. Right side is prostate tissue, and left side is surrounding tissue of the prostate. (B) Comparison of nNOS-positive area. Each box represents the average nNOS-positive area (green area) in surrounding tissue of prostate in each group. nNOS-positive area was measured using an image analyzer. Error bars show standard error. AL = alginate group; CD = CD133⁺ group; DAPI = 4′,6-diamidino-2-phenylindole; EX = excision group; HE = hematoxylin-eosin; SH = sham group.

cated by yellow arrows in the bottom row of panels in Figure 2A) were obvious in the SH, AL, and CD groups, they were hardly visible in the EX group. The value for the CD group ($7,390 \pm 1240 \ \mu m^2$) was significantly higher than the values for the EX ($1,350 \pm 340 \ \mu m^2$) and AL ($2,440 \pm 490 \ \mu m^2$) groups ($P < 0.01$). There was no significant differ-

ence between CD group and SH group ($8,670 \pm 940 \ \mu m^2$) (Figure 2B).

Blood Vessel Density in Surrounding Tissues of the Prostate

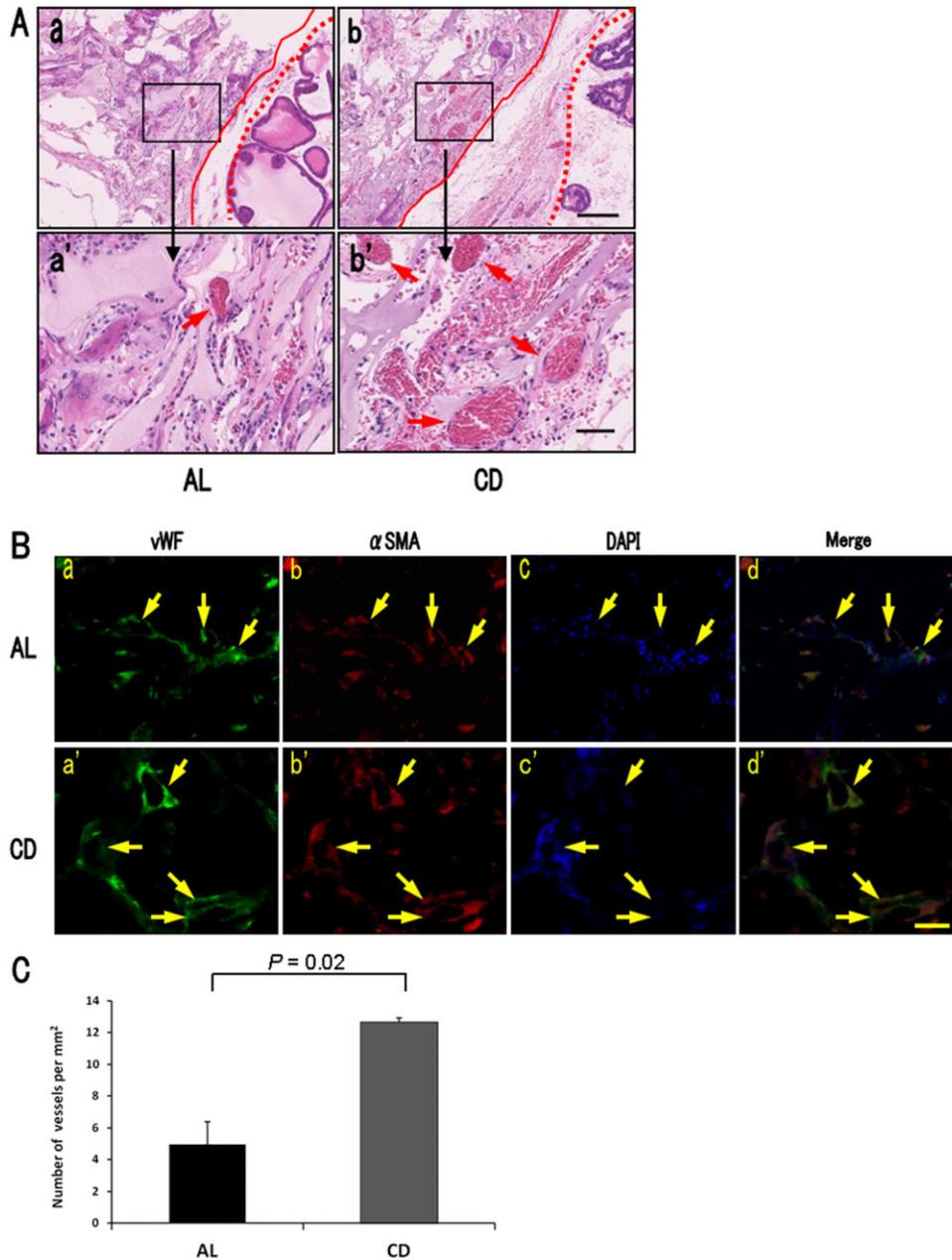Figure 3 shows micrographs of the prostate and its surrounding tissues in the AL and CD groups 12

Figure 3 Blood vessels in surrounding tissue of the prostate in AL and CD groups at 12 weeks. (A) Microscopic findings. Upper and lower row of panels are representative light micrographs showing HE-stained harvested tissues. A-a, b are divided into two regions by dotted lines. Right side is prostate tissue, and left side is surrounding tissue of the prostate. Continuous red lines show the alginate gel sponge sheet in the surrounding tissue of the prostate. Bar = 200 μm. Lower row of panels show magnifications of zones of A-a′ and A-b′. Bar = 50 μm. (B) Fluorescence micrograph showing von Willebrand factor (vWF) (green; B-a, a′), α-smooth muscle actin (αSMA) (red; B-b, b′), DAPI (blue; B-c, c′), and merge (B-d, d′). Upper panels are AL group, and lower panels are CD group. Bar = 100 μm. Abundant blood vessels (red parts and yellow arrows) were seen in the CD group. (C) Blood vessel density in groups AL and CD. Each box represents the average of blood vessel density. Error bars represent standard error. AL = alginate group; CD= CD133+ group; DAPI = 4′,6-diamidino-2-phenylindole; HE = hematoxylin-eosin.

weeks after surgery. Blood vessels were observed with HE staining (red arrows in Figure 3A) and immunofluorescence staining (yellow arrows in Figure 3B) in both groups. These blood vessels were also observed in alginate gel sponge sheet. The mean blood vessel density for 20 sections in the CD group (12.67 ± 0.25 per mm²) was significantly ($P = 0.02$) higher than it was in the

AL group (4.96 ± 1.27 per mm^2) (Figure 3C). Transplanted CD133$^+$ cells accelerated not only nerve regeneration but also blood structure improvement.

Differentiation of Transplanted Human-Derived CD133$^+$ Cells

The presence of HNA-positive cells was observed in the surrounding tissues of prostate at day 4 and 12 weeks later (yellow arrows in Figure 4A and white arrows in Figure 4B and C). Furthermore, HNA-vWF double-stained cells could be confirmed, although some HNA-positive cells were assimilated as vascular endothelial cells at day 4 and very few HNA-positive cells were incorporated into the blood vessels walls 12 weeks later (yellow arrows in Figure 4A). Neither HNA-nNOS double-stained cells nor HNA-S100 double-
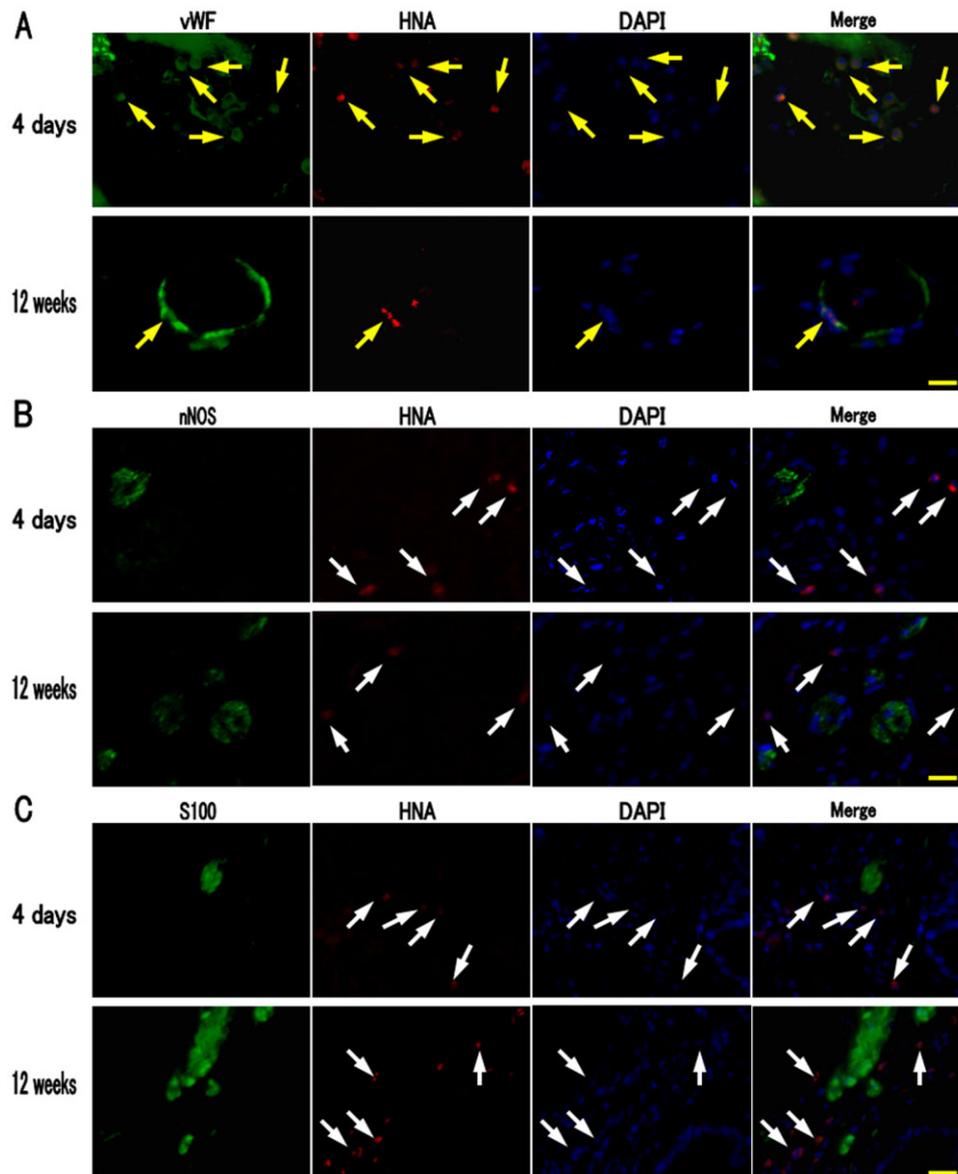

Figure 4 Differentiation of transplanted cells. (A) HNA (red), vWF (green), DAPI (blue), and merge at 4 days (upper row of panels) and 12 weeks (lower row of panels) were observed by immunofluorescence microscopy. HNA-positive cells were assimilated as vascular endothelial cells (yellow arrows). Bar = 20 μm. (B, C) HNA-positive cells were observed (white arrows). However, HNA-positive cells were not assimilated as neurons (B) and Schwann cells (C) at day 4 and at 12 weeks. Bar = 20 μm. DAPI = 4′,6-diamidino-2-phenylindole; HNA = human nuclear antigen; nNOS = neuronal nitric oxide synthase; vWF = von Willebrand factor.

stained cells could be confirmed at day 4 or 12 weeks later (Figure 4B and C). These results demonstrated the differentiation of human CD133+ cells into endothelial cells, although only a few cells were observed. On the other hand, the differentiation of human CD133+ cells into neuron cell or Schwann cell was not observed.

VEGF and NGF mRNA Expression in Alginate Gel Sponge Sheet

RT-PCR for the extracts from the alginate gel sponge sheets retrieved in the CD group revealed that the expression of mRNA for human GAPDH was evident but the expression of mRNA for human VEGF was not (Figure 5A). mRNA for rat NGF and rat VEGF was detected in both groups (Figure 5A), but quantitative RT-PCR found the amounts of mRNA for rat NGF and rat VEGF in the CD group to be significantly higher than those

Figure 5 Gene expression of alginate gel sponge sheets in AL and CD groups. (A) PCR products identified on agarose gel electrophoresis. (B) Relative levels of NGF and VEGF mRNA expression in AL and CD groups. Expression of β-actin mRNA was used as internal control. AL = alginate group; CD = CD133+ group; NGF = nerve growth factor; PCR = polymerase chain reaction; VEGF = vascular endothelial growth factor.

in the AL group (NGF: $P = 0.03$, VEGF: $P = 0.04$) (Figure 5B). While upregulation of intrinsic growth factors was observed, VEGF derived from human CD133+ cells was not observed.

Discussion

ED emerges as an important quality of life issue following radical prostatectomy because iatrogenic cavernous nerve injury may take place during the surgery. In the present study, we addressed this issue by investigating the effects of human CD133+ cells on the cavernous nerve regeneration in a rat model.

We found that the nNOS-positive area in the cell-treated rats was significantly more extensive than the nNOS-positive areas in the non-treated rats and alginate sheet alone-treated rats. Parallel to this finding, the ICP during electrical stimulation was significantly higher in the cell-treated rats than it was in the non-treated rats and was more marked in the cell-treated rats than it was in the alginate sheet alone-treated rats even though the difference between the cell-treated and alginate sheet alone-treated rats was not statistically significant. These findings suggest that the transplanted human CD133+ cells accelerated nerve regeneration, and this in turn resulted in functional recovery, represented in this rat model by an increased ICP.

With regard to the mechanism of nerve regeneration, it is unlikely that the CD133+ cells directly differentiated into nerve tissue, although they are reportedly able to differentiate into various cell types when placed in the appropriate conditions [8] [9] [10]. Endothelial cells are known to be important for neurogenesis. They have been reported to be a critical component of the neural stem cell niche, releasing soluble factors that stimulate the self-renewal of neural stem cells, inhibit their differentiation, and enhance their neuron production [11]. The importance of endothelial cells for neurogenesis is also indicated by the observation that the significantly better neurogenesis in the cell-treated rats was paralleled by excellent blood vessel formation. The transplanted human CD133+ cells are thought to have differentiated into endothelial cells because although some of the HNA-positive cells were also vWF positive, none reacted with nNOS or S100 antibodies. It is no wonder that the CD133+ cells differentiated not into nerve cells but into endothelial cells, because they are hematopoietic and are endothelial progenitors [12].
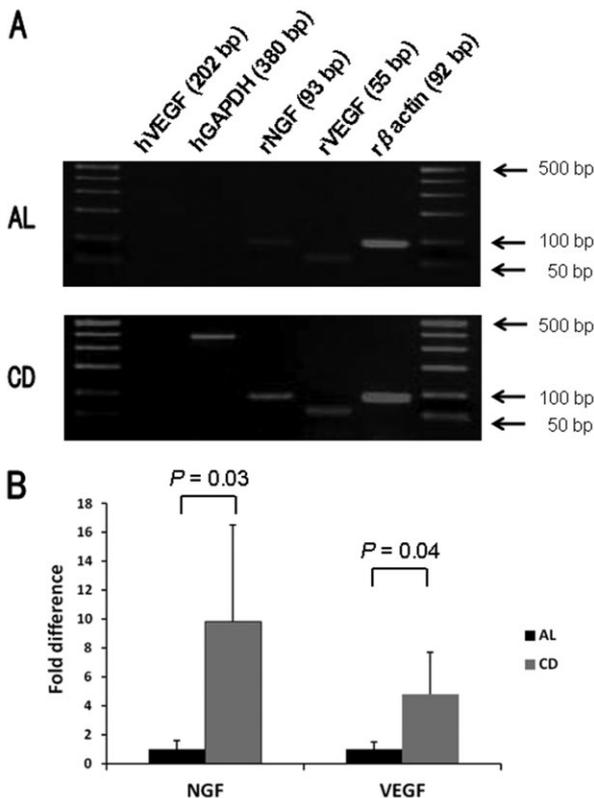
However, because most of the endothelial cells in the cell-treated rats were negative to HNA and therefore probably originated from the host rat, the endothelial cells resulting from the differentiation of transplanted CD133+ cells were not key players in the nerve regeneration in this study. Thus, the primary mechanism of nerve regeneration by CD133+ cells was neither that CD133+ cells directly differentiated into nerve cells nor that they stimulated neurogenesis indirectly by differentiating into endothelial cells. Instead, it is likely that CD133+ cells regenerated cavernous nerve through upregulation of endogenous VEGF and NGF and resulting stimulation of angiogenesis in the host rat because not human-derived but rat-derived VEGF and NGF were expressed in the extracts from the alginate gel sponge sheet and also because the amounts of these growth factors were significantly higher in the cell-treated rats than they were in the alginate sheet alone-treated rats.

Previous studies of cell therapy in cavernous nerve injury rat model, acute rabbit penile cavernosal injury model, or diabetic rat model suggested that paracrine mechanism of stem cells is important, although these studies used bone marrow-derived mesenchymal stromal cells (MSCs) [13], adipose tissue-derived stem cells (ADSCs) [14–16], or muscle-derived stem cells [17,18]. Also, recent experimental evidence obtained in endothelial progenitor cell therapy studies suggests that the injury site improvement elicited by transplanted cells may be mainly due to the release of multiple cytokines and chemokines rather than to cell differentiation because very few transplanted cells were found incorporated into the vascular structure [19–21].

VEGF is known to be an endothelial cell-specific growth factor that contributes to angiogenesis. It is also known to have both neurotrophic and neuroprotective effects [22] and to increase the number of proliferating Schwann cells [23]. Previous studies on the role of transplanted human CD133+ cells in a rat spinal cord injury model have, like the present study, found that the expression of rat VEGF or angiopoietine-1 increases significantly soon after the cells are transplanted [10,24]. The authors of the articles reporting those studies stated that the mechanisms of the upregulation of intrinsic angiogenic factor after CD133+ cells transplantation is unclear, but transplanted CD133+ cells might have been a trigger for the upregulation of growth factor [10,24]. Furthermore, it has been reported that Schwann cells secrete neurotrophic factors, such as NGF [25,26].

These findings suggest that transplanted CD133+ cells activate intrinsic growth factor and contribute to nerve regeneration.

We observed the expression of mRNA for NGF and VEGF in the alginate sheet-alone rats as well the cell-treated rats. Alginate gel itself has been reported to provide a favorable environment for Schwann cell migration and the growth of regenerating axons and to promote nerve regeneration in cat and rat sciatic nerve injury [27,28]. Furthermore, much better nerve regeneration had been found in collagen sponge and fibrin glue [28]. As cell infiltration into alginate gel occurs a few days after gel implantation [29], the NGF and VEGF mRNA found at 4 days in the alginate sheet alone-treated rats is thought to have originated from infiltrated cells.

Extracellular matrix and cytokines such as growth factors are essential to create new tissues [30]. CD133+ cells in alginate gel sponge sheets can induce these factors efficiently and are therefore potentially useful for cavernous nerve regeneration. Compared with previous studies using MSCs, ADSCs, skeletal muscle-derived cells, Schwann cells, collagen sponge, or alginate gel sheet, ICP/MAP ratio of this study is similar or superior, although there are differences in route of administration, injury method, and evaluation time [4–6,13–15,17,31]. Furthermore, there are few ethics issues relevant to autologous therapeutic agents because the cells are derived from human tissue. CD133+ cells thus appear to be one of the optimum sources of the agents useful for clinical setting. CD133+ cells can be isolated from bone marrow, peripheral blood, and umbilical cord blood easily. Especially, isolating CD133+ cells from peripheral blood is a more minimally invasive procedure than other procedures. There are, however, still some problems to overcome for clinical application and some limitations in this study. One of problems is that the number of CD133+ cells available is extremely limited [20]. This problem can be resolved by growth factor-driven ex vivo expansion of CD133+ cells [32]. The methods used in this study are promising for the future but we must investigate their safety and efficacy, and to achieve better nerve regeneration, must also further investigate the regeneration mechanism. One of limitations is that histological results in this study were obtained from two rats (four study nerves). Another limitation is that results of this study were founded in xenogeneic animal model. Recently, clinical researches that CD133+ cells implanted in patients undergoing coronary bypass

surgery were reported [33,34]. These researches may become useful for our field.

Conclusion

Our findings indicated that transplantation of human CD133+ cells is potentially useful for cavernous nerve reconstruction after operations such as radical prostatectomy.

Acknowledgments

Corresponding Author: Katsutoshi Miyamoto, MD, Department of Urology, Institute of Biomedical & Health Sciences, Hiroshima University. 1–2-3 Kasumi, Minami-ku, Hiroshima 734–8551, Japan. Tel: (81) 82-257-5242; Fax: (81) 82-257-5244; E-mail: sppw2d99@hyper.ocn.ne.jp

Conflict of Interest: The authors report no conflict of interest.

Statement of Authorship

Category 1
(a) Conception and Design
Katsutoshi Miyamoto; Shogo Inoue; Akio Matsubara
(b) Acquisition of Data
Katsutoshi Miyamoto; Shogo Inoue; Kanao Kobayashi; Mitsuru Kajiwara; Jun Teishima
(c) Analysis and Interpretation of Data
Katsutoshi Miyamoto; Shogo Inoue; Kanao Kobayashi; Mitsuru Kajiwara; Jun Teishima

Category 2
(a) Drafting the Article
Katsutoshi Miyamoto; Shogo Inoue; Jun Teishima; Akio Matsubara
(b) Revising It for Intellectual Content
Katsutoshi Miyamoto; Shogo Inoue; Jun Teishima

Category 3
(a) Final Approval of the Completed Article
Katsutoshi Miyamoto; Shogo Inoue; Akio Matsubara

References

1 Dubbelman YD, Dohle GR, Schröder FH. Sexual function before and after radical retropubic prostatectomy: A systematic review of prognostic indicators for a successful outcome. Eur Urol 2006;50:711–8.

2 Satkunasivam R, Appu S, Al-Azab R, Hersey K, Lockwood G, Lipa J, Fleshner N. Recovery of erectile function after unilateral and bilateral cavernous nerve interposition grafting during radical pelvic surgery. J Urol 2009;181:1258–63.

3 Kim ED, Nath R, Slawin KM, Kadmon D, Miles BJ, Scardino PT. Bilateral nerve grafting during radical retropubic prostatectomy: Extended follow-up. Urology 2001;58:983–7.

4 Hisasue S, Kato R, Sato Y, Suetomi T, Tabata Y, Tsukamoto T. Cavernous nerve reconstruction with a biodegradable conduit graft and collagen sponge in the rat. J Urol 2005;173:286–91.

5 May F, Matiasek K, Vroemen M, Caspers C, Mrva T, Arndt C, Schlenker B, Gais P, Brill T, Buchner A, Blesch A, Hartung R, Stief C, Gansbacher B, Weidner N. GDNF-transduced Schwann cell grafts enhance regeneration of erectile nerves. Eur Urol 2008;54:1179–87.

6 Matsuura S, Obara T, Tsuchiya N, Suzuki Y, Habuchi T. Cavernous nerve regeneration by biodegradable alginate gel sponge sheet placement without sutures. Urology 2006;68:1366–71.

7 Goussetis E, Theodosaki M, Paterakis G, Peristeri J, Petropoulos D, Kitra V, Papassarandis C, Graphakos S. A functional hierarchy among the CD34+ hematopoietic cells based on in vitro proliferative and differentiated potential of AC133+CD34(bright) and AC133(dim/-)CD34+ human cord blood cells. J Hematother Stem Cells 2000;9:827–40.

8 Tondreau T, Meuleman N, Delforge A, Dejeneffe M, Leroy R, Massy M, Mortier C, Bron D, Lagneaux L. Mesenchymal stem cells derived from CD133-positive cells in mobilized peripheral blood and cord blood: Proliferation, Oct4 expression, and plasticity. Stem Cells 2005;23:1105–12.

9 Kijima Y, Ishikawa M, Sunagawa T, Nakanishi K, Kamei N, Yamada K, Tanaka N, Kawamata S, Asahara T, Ochi M. Regeneration of peripheral nerve after transplantation of CD133+ cells derived from human peripheral blood. J Neurosurg 2009;110:758–67.

10 Fujioka Y, Tanaka N, Nakanishi K, Kamei N, Nakamae T, Izumi B, Ohata R, Ochi M. Magnetic field-based delivery of human CD133+ cells promotes functional recovery after rat spinal cord injury. Spine 2012;37:768–77.

11 Shen Q, Goderi SK, Jin L, Karanth N, Sun Y, Abramova N, Vincent P, Pumiglia K, Temple S. Endothelial cells stimulate self-renewal and expand neurogenesis of neural stem cells. Science 2004;28:1338–40.

12 Yin AH, Miraglia S, Zanjani ED, Almeida-Porada G, Ogawa M, Leary AG, Oweus J, Kearney J, Buck DW. AC133, a novel marker for human hematopoietic stem and progenitor cells. Blood 1997;90:5002–12.

13 Albersen M, Kendirci M, Van der Aa F, Lin G, Hellstrom WJ, Lue TF, Spees JL. Multipotent stromal cell therapy for cavernous nerve injury-induced erectile dysfunction. J Sex Med 2012;9:385–403.

14 Albersen M, Fandle TM, Lin G, Wang G, Banie L, Lin CS, Lue TF. Injections of adipose tissue-derived stem cells and stem cell lysate improve recovery of erectile function in a rat model of cavernous nerve injury. J Sex Med 2010;7:3331–40.

15 Piao S, Kim IG, Lee JY, Hong SH, Kim SW, Hwang TK, Oh SH, Lee JH, Ra JC, Lee JY. Therapeutic effect of adipose-derived stem cells and BDNF-immobilized PLGA membrane in a rat model of cavernous nerve injury. J Sex Med 2012;9:1968–79.

16 Nishimatsu H, Suzuki E, Kumano S, Nomiya A, Liu M, Kume H, Homma Y. Adrenomedullin mediates adipose tissue-derived stem cell-induced restoration of erectile function in diabetic rats. J Sex Med 2012;9:482–93.

17 Kovanecz I, Rivera S, Nolazco G, Vernet D, Segura D, Gharib S, Rajfer J, Gonzalez-Cadavid NF. Separate or combined treatments with daily sildenafil, molsidomine, or muscle-derived stem cells prevent erectile dysfunction in a rat model of cavernosal nerve damage. J Sex Med 2012;9:2814–26.

18 An G, Ji C, Wei Z, Chen H, Zhang J. The therapeutic role of VEGF-expressing muscle-derived stem cells in acute penile cavernosal injury. J Sex Med 2012;9:1988–2000.

19 Yoshiioka T, Ageyama N, Shibata H, Yasu T, Miasawa Y, Takeuchi K, Matsui K, Yamamoto K, Terao K, Shimada K, Ikeda U, Ozawa K, Hanazono Y. Repair of infarcted myocardium mediated by transplanted bone marrow-derived CD34⁺stem cells in a nonhuman primate model. Stem Cells 2005;23:355–64.

20 Ii M, Nishimura H, Iwakura A, Wecker A, Eaton E, Asahara T, Losordo DW. Endothelial progenitor cells are recruited to myocardium and mediate protective effect of ischemic preconditioning via "imported" nitric oxide synthase activity. Circulation 2005;111:1114–20.

21 Kinnaird T, Stabile E, Burnett MS, Shou M, Lee CW, Barr S, Fuchs S, Epstein SE. Local delivery of marrow-derived stromal cells augments collateral perfusion through paracrine mechanisums. Circulation 2004;109:1543–9.

22 Kunlin J, Yonghua Z, Yunjuan S, Xiao OM, Lin X, Greenberg DA. Vascular endothelial growth factor (VEGF) stimulates neurogenesis in vitro and in vivo. Proc Natl Acad Sci USA 2002;99:11946–50.

23 Sondell M, Lundborg G, Kanje M. Vascular endothelial growth factor has neurotropic activity and stimulates axonal outgrowth, enhancing cell survival and Schwann cell proliferation in the peripheral nervous systems. J Neurosci 1999;19:5731–40.

24 Sasaki H, Ishikawa M, Tanaka N, Nakanishi K, Kamei N, Asahara T, Ochi M. Administration of human peripheral blood-derived CD133⁺ cells accelerates functional recovery in a rat spinal cord injury model. Spine 2009;34:249–54.

25 Frostick SP, Yin Q, Kemp GJ. Schwann cells, neurotrophic factors, and peripheral nerve regeneration. Microsurgery 1998;18:397–405.

26 Stankoff B, Aigrot MS, Noël F, Wattilliaux A, Zalc B, Lubetzki C. Ciliary neurotrophic factor (CNTF) enhances myelin formation: A novel role for CNTF and CNTF-related molecules. J Neurosci 2002;22:9221–7.

27 Suzuki Y, Tanihara M, Ohnishi K, Suzuki K, Endo K, Nishimura Y. Cat peripheral nerve regeneration across 50 mm gap repaired with novel nerve guide composed of freeze-dried alginate gel. Neurosci Lett 1999;259:75–8.

28 Hashimoto T, Suzuki Y, Kitada M, Kataoka K, Wu S, Suzuki K, Endo K, Nishimura Y, Ide C. Peripheral nerve regeneration through alginate gel: Analysis of early outgrowth and late increase in diameter of regenerating axons. Exp Brain Res 2002;146:356–68.

29 Ohta M, Suzuki Y, Chou H, Ishikawa N, Suzuki S, Tanihara M, Suzuki Y, Mizushima Y, Dezawa M, Ide C. Novel heparin/alginate gel combined with basic fibroblast growth factor promotes nerve regeneration in rat sciatic nerve. J Biomed Mater Res A 2004;71:661–8.

30 Langer R, Vacant JP. Tissue engineering. Science 1993;60:920–6.

31 Kim Y, Miguel F, Usiene I, Kwon D, Yoshimura N, Huard J, Chancellor MB. Injection of skeletal muscle-derived cells into the penis improves erectile function. Int J Impot Res 2006;18:329–34.

32 Ohtsubo S, Ishikawa M, Kamei N, Kijima Y, Suzuki O, Sunagawa T, Higashi Y, Masuda H, Asahara T, Ochi M. The therapeutic potential of ex vivo expanded CD133⁺ cells derived from human peripheral blood for peripheral nerve injuries. J Neurosurg 2012;117:787–94.

33 Stamm C, Kleine HD, Choi YH, Dunkelmann S, Lauffs JA, Lorenzen B, David A, Liebold A, Nienaber C, Zurakowski D, Freund M, Steinhoff G. Intramyocardial delivery of CD133⁺ bone marrow cells and coronary bypass grafting for chronic ischemic heart disease: Safety and efficacy studies. J Thoracic Cardiovasc Surg 2007;133:717–25.

34 Forcillo J, Stevens LM, Mansour S, Prieto I, Salem R, Baron C, Roy DC, Larose E, Masckauchan D, Noiseux N. Implantation of CD133⁺ stem cells in patients undergoing coronary bypass surgery: Impact-CABG pilot trial. Can J Cardiol 2013;29:441–7.